Received: 27 November 2025 | Accepted: 31 March 2026

DOI: 10.1111/1365-2435.70352

Functional Ecology

RESEARCH ARTICLE

Wind, waves, wing loading and the flight energetics of giant petrels

Madeline E. Hallet[1] | Richard A. Phillips[2] | Ian J. Maywar[1] | Lesley H. Thorne[1]

[1]School of Marine and Atmospheric Sciences, Stony Brook University, Stony Brook, New York, USA

[2]British Antarctic Survey, Natural Environment Research Council, Cambridge, UK

Correspondence
Madeline E. Hallet
Email: madeline.hallet@stonybrook.edu

Funding information
National Science Foundation, Grant/Award Number: 2444342 and 79804; British Antarctic Survey

Handling Editor: David Gremillet

Abstract

1. Wind is a major factor driving seabird movement and energetics, the effects of which are modulated by morphology. Developments in tagging technology now make it possible to test predictions from aerodynamic theory about the effects of wind on flight performance in free-ranging birds. Waves are also thought to have a strong influence on seabird movement but have received less attention.
2. We investigated the interplay between wind, waves, and morphology and tested predictions of flight theory in giant petrels (*Macronectes* spp.), which show greater sexual size dimorphism than any other seabird. We quantified flapping rates as a proxy of energy expenditure using accelerometers deployed on northern giant petrels (*M. halli*; $n = 45$) and southern giant petrels (*M. giganteus*; $n = 48$) breeding at Bird Island, South Georgia in 2022 and 2023. Wind and waves experienced by birds tracked with Global Positioning System (GPS) loggers were integrated with ERA5 reanalysis data to assess how flapping rates and ground speeds, respectively, were influenced by wind and waves. Using generalized additive mixed models, we predicted the spatial distribution of suitable habitat for soaring based on wind and wave conditions.
3. Both wind and waves strongly influenced flight energetics; flapping rates decreased with increasing wind speed and swell height in all species and sexes. Together, wind and waves allowed giant petrels to reduce flapping rates by 76% to 91%. Wind also influenced the speed of travel; ground speed increased with wind speed in tail- and crosswinds, but generally decreased with wind speed in headwinds.
4. Male giant petrels had higher wing loadings, and as predicted by flight theory, required higher air speeds for soaring flight and had higher flapping rates than females. Potential soaring habitat was much more limited for male than for female giant petrels, suggesting that differences in flight energetics between sexes may contribute to sexual segregation in foraging areas.
5. Our results demonstrate how morphology, wind and waves combine to influence the flight energetics of giant petrels. Understanding the interactions among these

factors is central to understanding environmental drivers of seabird distribution and to predicting responses to continued climate change.

KEYWORDS
aerodynamic performance, dynamic soaring, flap, morphology, sexual size dimorphism, swell, wave slope soaring

1 | INTRODUCTION

Bird flight has fascinated humans for centuries (Baines, 1889; da Vinci, 1505; Rayleigh, 1883), and wind is increasingly recognized as a major factor influencing bird flight and energetics (Kemp et al., 2010; Pennycuick, 1978; Safi et al., 2013; Thorne et al., 2023). The development of quantitative flight theory focusing on the physics and aerodynamics of bird flight since the 1960s has provided testable hypotheses about flight performance relative to wind speed and direction (Cone, 1964; Hedenström, 2003; Parrott, 1970; Pennycuick, 1978; Tucker & Parrott, 1970). Over the last 10–15 years, technological advances have provided empirical data at sufficient resolution to test many of these predictions, greatly improving our mechanistic understanding of the impacts of wind on bird flight energetics (Conners et al., 2021; Kogure et al., 2016; Schoombie et al., 2023; Spivey et al., 2014).

Wind can influence the cost and speed of travel, and seabirds have both morphological and behavioural adaptations allowing them to use wind to decrease flight costs (Collins et al., 2020; Spivey et al., 2014; Suryan et al., 2008). Albatrosses (Diomedeidae) and some petrels (Procellariidae) employ dynamic soaring, which involves tacking back and forth in an S-shaped trajectory, exploiting energy from the wind shear gradient for efficient long-distance movement with minimal flapping (Pennycuick, 1982; Richardson, 2011; Richardson et al., 2018). Although waves can also influence seabird movement and energetics, this has received little research attention (Suryan et al., 2008; Thorne et al., 2023). Wave slope soaring is used by various species including albatrosses, where birds fly ahead of a moving wave and use the uplift generated by air rising above the crest to gain altitude, allowing them to soar in the direction of wave propagation with minimal energetic cost (Pennycuick, 1982; Richardson, 2011; Stokes & Lucas, 2021; Wilson, 1975). The direction of wind and waves also influences dynamic soaring (Pennycuick, 1982; Richardson, 2011; Richardson et al., 2018; Spivey et al., 2014; Suryan et al., 2008; Wakefield et al., 2009; Weimerskirch et al., 2012). Seabirds may exploit energy from wind and waves additively to reduce the cost of flight, but there are few quantitative studies that directly quantify this relationship to date (Maywar et al., 2025; Suryan et al., 2008). Understanding the mechanistic links between wind, waves and dynamic soaring in seabirds is key to understanding their distributions, and constraints on their distribution.

Flight theory explores how seabird flight styles and manoeuvrability are shaped by morphology, which modulates the effect of wind and waves on energetics (Pennycuick, 2008; Suryan et al., 2008; Thorne et al., 2023). Birds that use dynamic soaring have high aspect ratios—the ratio of wing length to mean wing chord (i.e. mean wing width)—which provide greater lift and less drag, allowing the use of dynamic soaring in environments with high wind (Pennycuick, 2008). Wing loading ($N\,m^{-2}$)—body weight per unit wing area—influences minimum airspeeds, such that birds with higher wing loadings need higher airspeeds to stay aloft while gliding (Pennycuick, 2008). Body size and wing morphology can be used to predict flight performance, for example, in theoretical studies, the best glide speed (V_{bg}) is the airspeed at which the ratio of forward speed to sinking velocity reaches its maximum, and the stalling speed (V_s) is the minimum speed at which the wing can generate enough lift to support the weight of the bird, both of which represent gliding efficiency (Pennycuick, 2008). Although stalling speed and best glide speed do not relate directly to wind speed, the former influences the air speed and therefore provides an indication of the wind speeds required for gliding flight (Richardson, 2018; Spear & Ainley, 1997b).

While a considerable body of theory addresses links between morphology, energetics and the use of wind and waves by seabirds (Bousquet et al., 2017; Pennycuick, 2008; Richardson, 2011; Sachs, 2005; Stokes & Lucas, 2021), few studies have tested the resulting predictions using empirical data (Kempton et al., 2022; Schoombie et al., 2023; Spear & Ainley, 1997a; Suryan et al., 2008; Wakefield et al., 2009). The miniaturization and proliferation of accelerometers have greatly advanced our ability to infer flight patterns and energy expenditure, and the opportunity to better understand how morphology influences flight energetics, especially in relation to wind and waves (Collins et al., 2020; Conners et al., 2021; Schoombie et al., 2023; Spivey et al., 2014). Giant petrels (*Macronectes* spp.) provide an exemplary case study for assessing these relationships. There are two morphologically similar species: The southern giant petrel (*M. giganteus*) has slightly higher wing loadings than the northern giant petrel (*M. halli*), and both use dynamic soaring and wave slope soaring (Hunter, 1984; Obst & Nagy, 1992; Pennycuick, 1982; Warham, 1977). They show marked sexual segregation in foraging distribution; males primarily scavenge on carrion from penguins and pinnipeds on land for much of the breeding season, whereas females predominantly feed at sea (Granroth-Wilding & Phillips, 2019; Hunter, 1983; Phillips et al., 2011; Reisinger et al., 2020; Thiers et al., 2014). There is pronounced sexual dimorphism; males are 20–30% heavier than females, which is the greatest sexual size dimorphism among seabirds (González-Solís, 2004; Hunter, 1984). This sexual dimorphism likely affects energetics of travel relative to wind, but

the role of wind in determining the sexual segregation in at-sea habitat use has not been assessed in detail.

Here, we test predictions from flight theory based on morphology and associated aerodynamic metrics for giant petrels of both species, and assess the role of wind and waves in driving sexual segregation. Our specific objectives were to: (1) test whether aerodynamic performance based on wing morphology and observed flapping rates (flaps per hour) differs among species and sexes; (2) assess how wind and waves influence energy expenditure (using the number of flaps as a proxy); (3) evaluate the effects of wind speed, wind direction, and wing loading on ground speed; and (4) examine the role of morphology in mediating relationships between wind, waves and energy expenditure. We expected that male giant petrels would generally have higher flapping rates than females, and that southern giant petrels would have higher flapping rates than northern giant petrels, due to their higher wing loading but similar aspect ratios. We postulated that flapping rates would decrease at higher wind speeds and swell heights (which may reflect opportunities for dynamic soaring or wave slope soaring) and that the sex (males) and species (southern giant petrel) with higher wing loadings would show higher flapping rates for a given wind speed or swell height. We also expected that giant petrels would have the highest ground speeds in tailwinds, that ground speed would increase with wind speed, and that the sex and species with higher wing loadings would show the highest ground speeds in those conditions. We discuss our results in the context of explaining habitat use and accessibility, including the marked sexual segregation in giant petrels during the breeding season.

2 | METHODS AND MATERIALS

2.1 | Study site and tag deployment

Breeding giant petrels were tracked at Bird Island, South Georgia (54°00′ S, 38°03′ W) during the incubation and brood-guard periods in November 2022 to early March 2023 (Figure 1). Eggs of northern and southern giant petrels are laid in late September to early October, and late October to late November, respectively, and parents take turns incubating the egg or brooding small chicks and foraging for multiple days at sea.

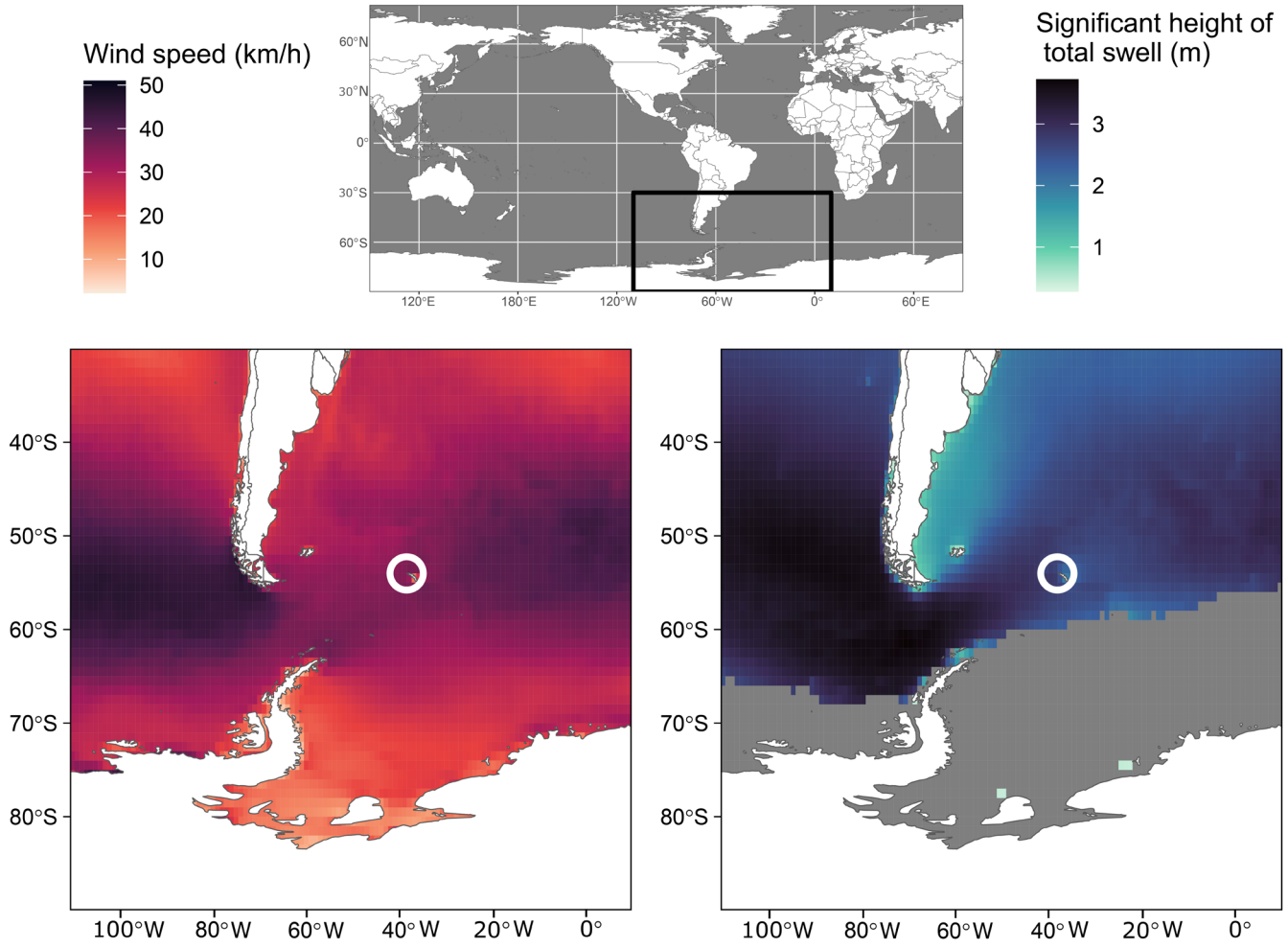

FIGURE 1 Location of the study area (top panel), study site (Bird Island; white circle) and maps of regional wind speeds (bottom left panel) and swell heights (bottom right panel) during the incubation and brood-guard periods of giant petrels (October, 2022–February, 2023). Grey shading indicates areas with no wind or swell data due to the presence of sea ice.

A tri-axial accelerometer (AXY5 or one of two sizes of AGM loggers, Technosmart, Italy; 13 g, 31 g or 44 g) and an archival GPS logger (CatLog GPS tag, Perthold Engineering, USA; 22 g) were attached to the central dorsal contour feathers using Tesa® tape (Germany), and a GLS-immersion logger (C330, Migrate Technology, UK; 3.3 g) fitted with a cable tie to a plastic ring was attached to the tarsus of 30 male and 30 female giant petrels of each species in each breeding stage ($n = 120$ deployments). Accelerometers were attached so that the x, y and z-axes aligned with the surge, sway and heave axes of the bird, respectively (see Conners et al., 2021). The mean maximum combined weight of the tags corresponded to 1.5% and 2.0% of the mean body mass of male and female giant petrels, respectively, which is well below the 3% threshold of body mass at which effects of devices tend to be more apparent in large seabirds (Phillips et al., 2003). Accelerometers sampled at a rate of 25 Hz; GPS tags were set to take a fix at ~5-min intervals; GLS-immersion loggers tested for immersion every 3 s and stored every change of state from wet to dry and vice versa that lasted ≥6 s. Birds were recaptured and devices removed at the end of a single foraging trip. One or more devices were lost from the feathers or malfunctioned on 15 northern giant petrels and 12 southern giant petrels, and so these individuals were excluded from the analysis. Field protocols were approved by the Stony Brook University Institutional Animal Care and Use Committee (IACUC, protocol number 1473497_TR001), and by the British Antarctic Survey Animal Welfare and Ethical Review Body (AWERB, permit number 1080), and carried out under a Regulated Activity Permit (RAP, permit number 2022/032) from the Government of South Georgia and the South Sandwich Islands.

2.2 | GPS and accelerometer data processing

Accelerometer data were pre-processed in MATLAB using the Signal Processing Toolbox (version 24.1) and in R. Flapping flight is energetically costly (Butler, 1991), and the number of flaps is considered to be a good proxy for energy expenditure in other large seabirds that use dynamic soaring (Conners et al., 2024). We therefore calculated the flapping rates (flaps per hour) from the accelerometer data. Following the methodology of Schoombie et al. (2023), we cleaned the raw accelerometer signal in the heave axis in order to detect flaps using a LULU operator (Lotz & Clilverd, 2019). The upper-limit band-width, m, was changed from 8 (the sampling frequency of 25 Hz, divided by 3 Hz, the flapping frequency of the wandering albatross (*Diomedea exulans*); Sato et al., 2009; Schoombie et al., 2023) to 4 (25 Hz divided by 9 Hz, the estimated flapping frequency of giant petrels, which is approximately 3–4 times greater than that of the wandering albatross; Obst & Nagy, 1992).

The GPS data at ~5-min intervals were pre-processed in R and then resampled at 10-min intervals in order to overcome slight inconsistencies in sampling rates. Using the moveHMM package (version 1.9; Michelot et al., 2016) in R, we used Hidden Markov Models (HMMs) to assign bird behavioural states in each 10-min interval as sitting, foraging, or commuting. Immersion data were also binned into 10-min intervals to differentiate between periods spent on the water as opposed to flying. These data were then summarized by hour to examine flapping rates relative to wind and waves (see below), focusing on commuting; if any location within the hour was classified by the HMM as sitting or foraging, those hours were excluded from further analysis. We excluded locations on or in close proximity to the colony using a 20 km buffer around South Georgia in the tidyterra package (version 0.6.1; Hernangómez, 2023). As a result, the number of deployments used in the models differed slightly from the total number of successful deployments. The final number of deployments included in analyses is described in Table S1. All data used to produce models are available from the Dryad Digital Repository (Hallet et al., 2026).

2.3 | Environmental data

Wind and wave data were obtained from the fifth generation European Centre for Medium-Range Weather Forecasts (ECMWF) analysis for global climate and weather (ERA5) online database (https://cds.climate.copernicus.eu/datasets; Copernicus Climate Change Service, 2023; Hersbach et al., 2023). We calculated wind speed and direction from the u and v wind components at 10 m altitude. Wave data were the significant height (m) of total swell (hereafter referred to as swell height). The resolution of wind and wave data were 0.25° by 0.25° and 0.5° by 0.5°, respectively, both by hour.

2.4 | Replication statement

Scale of inference	Scale at which the factor of interest is applied	Number of replicates at the appropriate scale
Species and sex	Species and sex	22 female northern giant petrels, 23 male northern giant petrels, 24 female southern giant petrels, 24 female northern giant petrels

2.5 | Analyses of aerodynamic performance

To calculate metrics of aerodynamic performance, we determined wing morphometrics from two male and two female northern giant petrels, and three male and three female southern giant petrels (all adults) found freshly dead on land at Bird Island or mainland South Georgia, or killed in fisheries in surrounding waters in summers 2017/18, 2018/19 and 2019/20. Photographs were taken from the dorsal side of the extended right wing and body, and a wing ruler for scale. The outline of the right wing plus half the area between the wings (root chord to the mid-point of the body) was digitized, and the area calculated using DotDotGoose software (http://cbc.amnh.org). The distance from the wing tip to the mid-point of the

body was also measured in DotDotGoose. Other measurements of flight morphology are available in the literature but often unreliable as age is unknown and body mass can fluctuate substantially depending on breeding stage and stomach contents. To overcome the latter, we calculated wing loading based on double the digitized area of the right wing and back of the dead birds, and the mean masses during the brood-guard stage in summer 2000/01 at Bird Island of 8 female and 15 male southern giant petrels, and 14 female and 13 male northern giant petrels. We then used these values as inputs in computer program *Flight* (version 1.24; Pennycuick, 2008). As a metric of aerodynamic performance, we calculated the stalling speeds of each species and sex, which represent the minimum airspeed needed to sustain flight and maintain altitude. We also calculated the best glide velocity of each species and sex to represent the airspeed at which a bird can cover the greatest air distance for a given loss of height (Pennycuick, 2008). For the stalling speed, higher values indicate higher air speeds required for soaring flight, which we hypothesize can result in lower energetic costs of flight due to reductions in flapping rates during soaring. The stalling speeds (V_S) were calculated using the following equation:

$$V_S = \left[\frac{2mg}{\rho S_W C_{LMax}}\right]^{1/2}$$

where m is bird mass (kg), g is acceleration due to gravity (9.81 $m\,s^{-2}$), ρ is the density of air at sea level (1.23 $kg\,m^{-3}$), S_W is wing surface area (m^2), and C_{Lmax} is the maximum lift coefficient (1.8 for birds adapted to gliding flight; Pennycuick, 2008).

2.6 | Effect of wind speed and swell height on flapping rates

We constructed generalized additive mixed models (GAMMs) using the mgcv package in R (version 1.9–1; Wood, 2017) to analyse the relationship between flapping rates and wind speed and swell height, running separate models for each species and sex. These involved assessing the independent effects of wind speed and swell height, respectively, and then modelling the two variables together to assess their additive effects. Individual was included as a random effect in all models to account for repeated measures. Here we focus only on the magnitude of wind and waves (wind speed and swell height), rather than the direction, to first examine implications for spatial distribution and habitat use; including direction of wind and waves requires understanding the heading of the birds relative to these factors, and therefore makes it difficult to assess how wind and waves relate generally to the spatial distribution of giant petrels (section 2.8). Separate models examining the relationship between flapping rates and wind speed and wind direction in female giant petrels are described in section 2.7. GAMMs were fitted using a negative binomial distribution with a log link function, and REML estimation. We used three knots for the wind and wave variable smooths, and the number of knots equal to the number of individuals for the random effect smooth. Following Maywar et al. (2025), we used forward model selection and ran four different models to select the best model for assessing the impacts of wind and waves on flapping rates: wind speed (Model I), swell height (Model II), both wind speed and swell height (Model III), and a null model that only included individual as a random effect. Models I and II incorporated a thin plate regression spline, and Model III incorporated a full tensor product smooth for the wind and swell terms to account for potential interactions as well as the different scales over which variables were measured. We also plotted the predicted flapping rates from Model III in relation to wind or swell, with the explanatory variable held at the median value experienced by each sex and species during flight, to visualize the individual effects of wind speed and swell height on flapping rates.

We quantified the energetic savings that giant petrels gain from exploiting wind and waves using the methods of Maywar et al. (2025). Briefly, we defined the energy savings as the percentage reduction in flapping rate, calculated as the difference between the maximum and minimum flapping rates predicted from the model (95th and 5th quantile, respectively) divided by the maximum flapping rate.

In order to compare energetic costs of flight in wind and waves between sexes, we applied the best model (Model III; see results) to predict flapping rates for male giant petrels if they travelled along the same tracks as females (i.e. if they experienced the same wind and wave conditions), and, similarly, predicted flapping rates for female giant petrels if they were to travel on the same tracks as males. We then compared the predicted male flapping rates with the predicted female flapping rates using paired Wilcoxon signed-rank tests.

2.7 | Effects of wind speed and direction on ground speed and flapping rates

To evaluate how average ground speed and flapping rates in giant petrels varied relative to wind speed and wind direction, we also calculated the angle between bird heading and the wind direction on a 0–180° scale such that 0° represents a direct tailwind (as wind direction describes the direction of origin of the wind) and 180° represents a direct headwind. We then categorized flight as tailwind (0–60°), crosswind (60–120°) or headwind (120–180°). We calculated the average ground speed in each hour by measuring the distance travelled between each 10-min GPS fix and taking the average speed of all 10-min time bins within each hour to match the hourly resolution of the environmental data.

To assess how ground speed and flapping rates, respectively, are influenced by wind speed and wind direction in giant petrels, we used GAMMs to model the interaction between wind speed and wind direction (tail-, cross- and headwinds), with individual included as a random effect. Due to the smaller sample size and higher error in the models for male giant petrels (see results), we modelled these relationships for females only. To visualize the effects of wind direction and wind speed on ground speed, we plotted the average

ground speed relative to wind speed for tailwinds, crosswinds and headwinds.

We also quantified the proportion of time that giant petrels spent flying in tail-, cross-, and headwinds, separately for each species and sex. Within each relative wind direction, we further quantified the proportion of time spent flying in low, medium and high wind speeds, defined as the 1/3 and 2/3 quantiles of the distribution of wind experienced by all species and sexes in the study.

2.8 | Assessment of suitable habitat for soaring

We generated maps of potential soaring habitat for giant petrels to visualize regions where wind and wave conditions would allow for energetically efficient flight based on our models. To do this, we first calculated the theoretical stalling speed for giant petrels based on morphology of each species and sex. We assumed that wind speeds would need to be above the stalling speed value for efficient gliding and dynamic soaring, and then used our model of flapping rate relative to wind speed and swell height to identify the flapping rate associated with this wind speed (hereafter referred to as maximum flapping rate during soaring). For example, for female northern giant petrels, we calculated the stalling speed from morphological data as 35.76 km/h (Table 1). We then calculated that the flapping rate was at a maximum of 2086 flaps per hour at this wind speed using our models (see Results, Figure 3). We recognize that movement can be facilitated by wave slope soaring in low wind conditions, that wind and swell can be used additively to reduce flapping, and that the maximum flapping rate for soaring can occur at combinations of wind and swell where the wind speed is less than the stalling speed. We therefore used our model of flapping behaviour relative to both wind and waves (see Results, Figure 3) to identify the range of wind and swell conditions that would allow for a flapping rate below the calculated maximum during soaring. We identified how often wind and wave conditions were sufficient to enable soaring in each grid cell of the study area (defined as the minimum and maximum latitude and longitude, respectively, travelled by all birds in the study; Table S4) as a proportion of hours during the middle month of incubation for each species (i.e. when birds are least constrained during breeding); November for northern giant petrels, and December for southern giant petrels. We plotted the resulting data (proportion of time that wind and wave conditions allow for soaring) to visualize regions that are particularly suitable for energetically efficient flight in giant petrels. Due to the limited sample size and higher error in the models for male northern giant petrels (see Results), this analysis focused on comparisons between females of each species, and between sexes in southern giant petrels, respectively.

3 | RESULTS

3.1 | Aerodynamic performance

Males were 43% and 41% heavier than females in northern and southern giant petrels, respectively, during the brood-guard period at Bird Island (Table 1). Based on those body masses and wing areas of birds found dead or killed in fisheries, wing loadings of males were 15% and 16% greater than females in northern and southern giant petrels, respectively. Mean masses of each sex were similar across species, but mean wing loading was 5% greater in male and 4% greater in female

TABLE 1 Mass, wing morphology, observed flapping rates, ground speeds and predicted aerodynamic performances of male and female giant petrels.

Sex and species	Male northern giant petrel	Female northern giant petrel	Male southern giant petrel	Female southern giant petrel
Mass ± SD (kg)	4.77 ± 0.30	3.33 ± 0.26	4.72 ± 0.49	3.34 ± 0.32
Wingspan (m)	2.18	1.95	2.11	1.84
Wing area (m^2)	0.37	0.30	0.35	0.29
Aspect ratio	12.78	12.72	12.78	11.83
Wing loading ($N\,m^{-2}$)	125.61	109.22	132.08	113.86
Stalling speed (m/s; km/h)	10.65; 38.35	9.93; 35.76	10.92; 39.32	10.14; 36.51
Minimum sink speed (m/s)	0.55	0.52	0.57	0.56
Best glide velocity (m/s; km/h)	14.40; 51.84	13.50; 48.60	14.70; 52.92	14.00; 50.40
Maximum flapping rate (flaps/h)	5837	7654	8818	8214
Mean flapping rate ± SE (flaps/h)	2239 ± 136	1620 ± 43.20	2622 ± 99.30	1921 ± 49.70
Mean ground speed ± SE (km/h)	38.40 ± 0.97	37.90 ± 0.37	46.70 ± 0.73	40.70 ± 0.38

Note: Minimum sink speed and best glide velocity were calculated from the computer program *Flight* (version 1.24; Pennycuick, 2008).

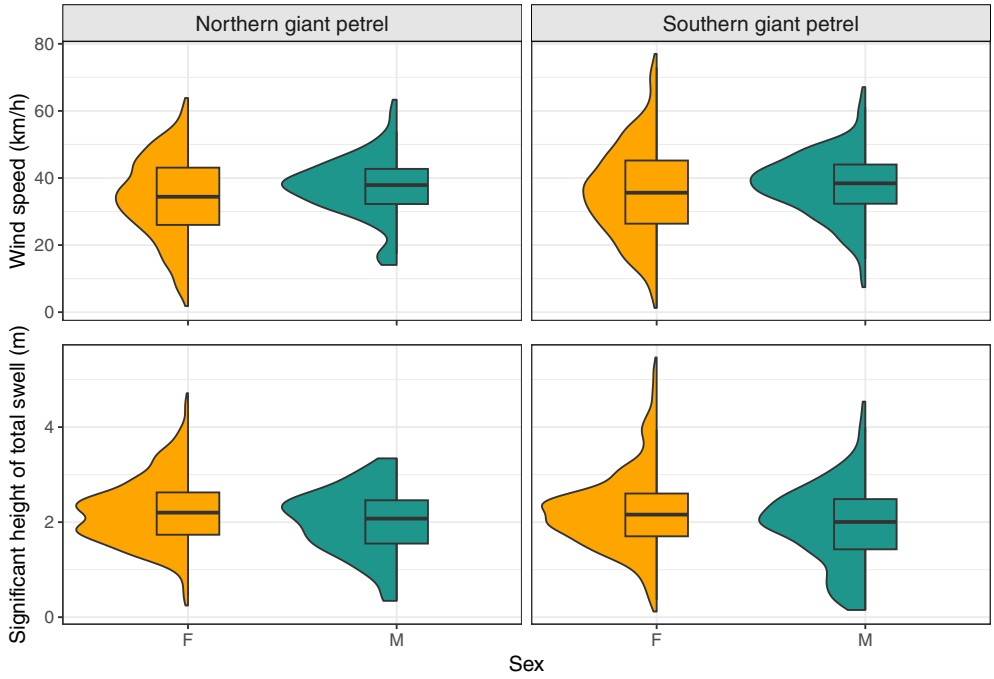

FIGURE 2 Box/violin plots of the wind and swell conditions experienced during commuting flight by northern and southern giant petrels tracked during incubation and brood-guard in November 2022 to early March 2023 at Bird Island (South Georgia).

southern than northern giant petrels. In each species, males had marginally higher stalling speeds and higher best glide velocities than females (Table 1). Stalling speeds and best glide velocities were higher for both sexes in southern giant petrels than northern giant petrels.

3.2 | Wind and swell experienced by giant petrels

The median wind speed along tracks was similar across species and sexes, but females of both species experienced low winds (< 20 km/h) for ~14% of the foraging trips, and male northern and male southern giant petrels for only ~7% and ~3% of foraging trips, respectively (Figure 2). The median swell height along tracks was also similar across species and sexes, but male southern and northern giant petrels experienced lower swell heights (<1 m) for 16% and 6% of foraging trips, and female southern and northern giant petrels for 5% and 2% of foraging trips, respectively. At the other end of the spectrum, high swell conditions (>3.3 m) were experienced by female northern giant petrels for 8% of foraging trips, and very rarely by male northern giant petrels, and even higher swells (>4 m) were also more likely to be experienced by female than male southern giant petrels (4% and 1% of foraging trips, respectively). Between species, southern giant petrels of either sex experienced higher maximum wind speeds and swell heights than northern giant petrels of either sex. Male and female northern giant petrels experienced wind speeds over 60 km/h for <1% and 1% of foraging trips, respectively, while male and female southern giant petrels experienced wind speeds over 60 km/h for 2% and 4% of foraging trips, respectively.

All species and sexes spent the most time in crosswinds, followed by tailwinds, and spent the least amount of time in headwinds (Figure S1). While in headwinds, all species and sexes spent the least amount of time in high wind speeds (Figures S2 and S3). Patterns in time spent in different swell directions were less clear in all species and sexes (Figure S1).

3.3 | Impacts of wind speed and swell height on flapping rates

On average, within each species, males had significantly higher flapping rates than females (Wilcoxon rank sum test, $p < 0.001$, Dunn-Šidák correction), and within each sex, southern giant petrels had higher flapping rates than northern giant petrels (significant difference between female southern giant petrels and female northern giant petrels only, Wilcoxon rank sum test, $p < 0.001$, Dunn-Šidák correction; Table 1). The best model for all species and sexes based on delta AICc was Model III, which included both wind speed and swell height (Table S2). Hereafter, results are those from this model. For both species and sexes, flapping rates decreased with increasing wind speeds and swell heights (Figure 3). At lower wind speeds (<30 km/h), giant petrels had low flapping rates only when swell was high (>3 m). However, when wind speeds were sufficiently high (>40 km/h in female giant petrels, >50 km/h in male giant petrels), flapping rates were low across swell heights.

The predicted flapping rates with swell height and wind speed set to their median values indicated that flapping rates decreased with increasing wind speed and swell height, respectively (Figure 4). At wind speeds lower than 5 km/h, flapping rates were considerably higher in female southern than northern giant petrels but decreased to a similar rate at wind speeds of ~60 km/h for both species. Female

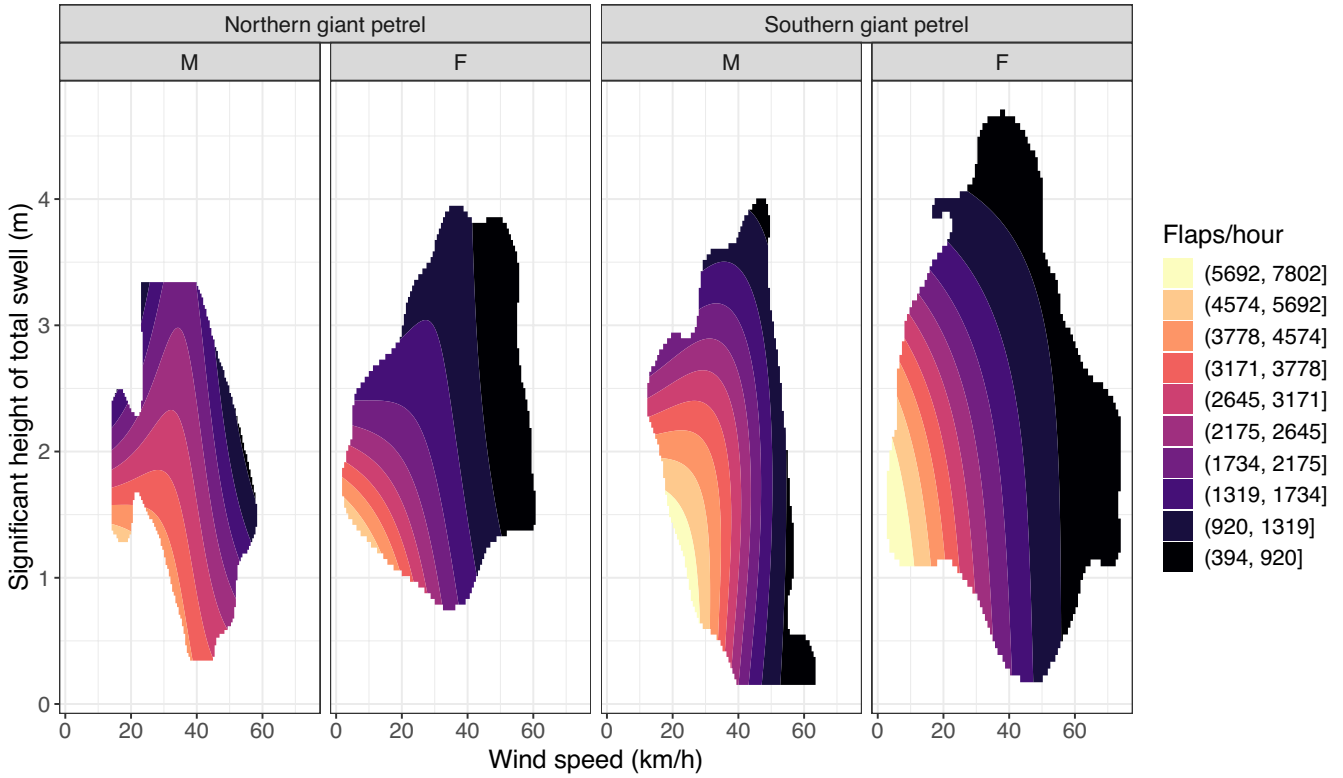

FIGURE 3 Flapping rate predicted using a generalized additive model full tensor product smooth of wind speed and swell height (Model III) fitted to northern and southern giant petrels tracked during the incubation and brood-guard periods in November 2022 to early March 2023 at Bird Island (South Georgia). Outputs are confined to the 95% kernel density estimate of the predictor variable space in order to focus on typical environmental conditions.

northern and southern giant petrels both had a maximum flapping rate in low swells (<1 m), which decreased to a minimum flapping rate at swell heights over 4 m (over 5 m in female southern giant petrels). Together, wind and waves resulted in reductions in flapping rates of 91% and 88% for female and male southern giant petrels, and of 89% and 76% for female and male northern giant petrels, respectively.

Within species, male giant petrels exhibited higher flapping rates than females in most wind speeds and swell heights, although these generally converged at similarly low values in high wind or wave conditions. Male giant petrels of both species had high flapping rates at wind speeds below ~30 km/h, which decreased with increasing wind speeds (Figure 4). Male northern giant petrels showed a general decline in flapping rates with increasing swell height, whereas male southern giant petrels showed declines in flapping rates at swell heights greater than ~2 m. The relationship between wind or waves and flapping rate was less clear for male northern giant petrels than for females or either sex of southern giant petrels and showed comparatively high error (Figure 4), likely due to the smaller sample size (Table S1).

3.4 | Effects of wind speed and direction on ground speed and flapping rates

Ground speed generally increased with wind speed in tail and crosswinds, but generally decreased with wind speed in headwinds, although these trends were less clear for male northern giant petrels (Figure 5). Male southern giant petrels showed significantly higher average ground speeds than female southern giant petrels (Wilcoxon rank sum test, $p < 0.001$, Dunn-Šidák correction), but there was no significant difference in average ground speeds experienced between male and female northern giant petrels (Table 2). Within each sex, southern giant petrels also had significantly higher average ground speeds than northern giant petrels (Wilcoxon rank sum test, $p < 0.001$, Dunn-Šidák correction). In all species and sexes except male northern giant petrels, the highest ground speeds were experienced in strong tailwinds.

Females of both giant petrel species showed decreases in flapping rates with increasing wind speed while flying in tailwinds and crosswinds, and slower flapping rates in tailwinds than crosswinds (Figure S4). In headwinds over ~20 km/h, female northern giant petrels showed declining flapping rates with wind speeds, and somewhat higher flapping rates than in tail and crosswinds. In contrast, in headwinds over ~20 km/h, female southern giant petrels showed flapping rates that were considerably higher than in tail and crosswinds.

3.5 | Predicted flapping rates

In all comparisons of predicted flapping rates between sexes, female giant petrels had lower predicted average flapping rates than

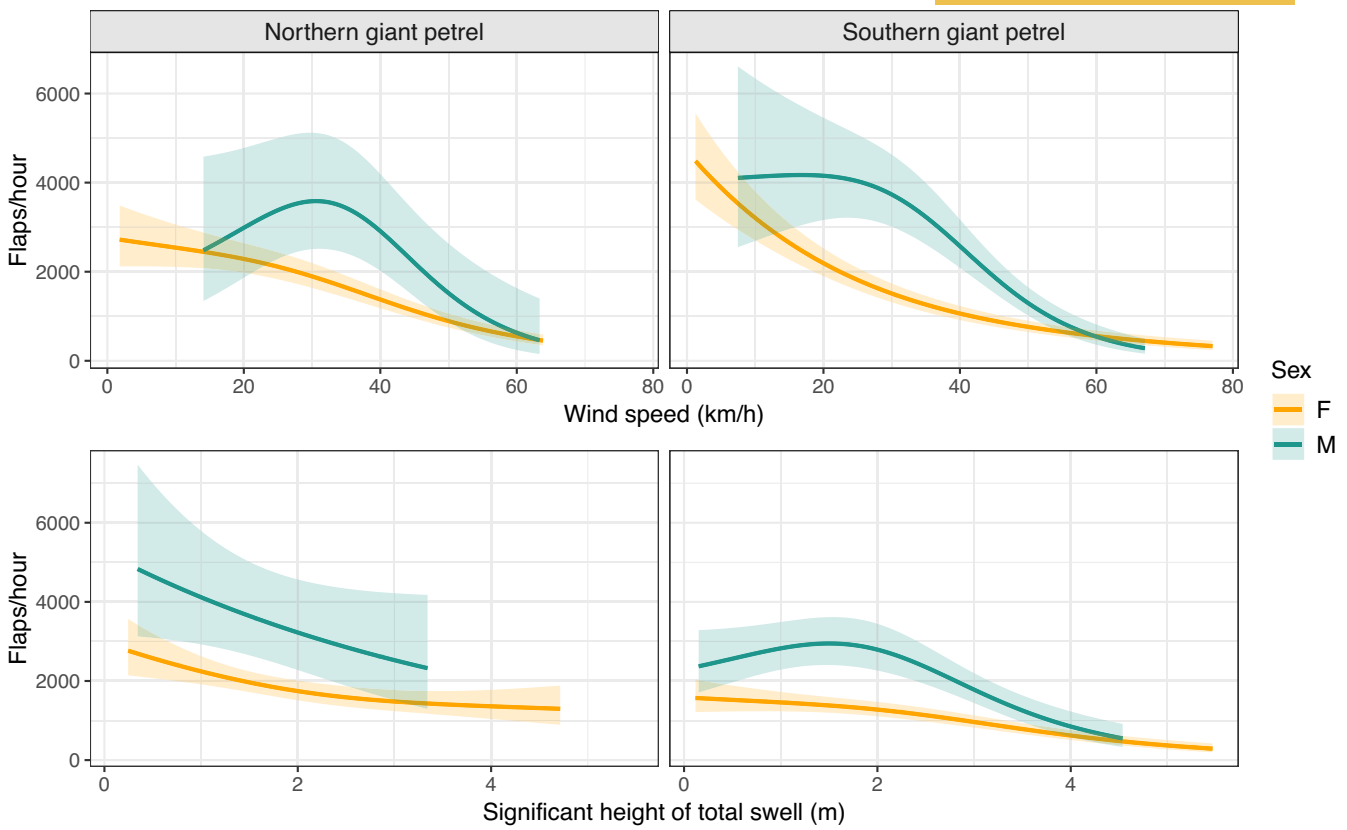

FIGURE 4 Flapping rates predicted from wind and waves (Model III) of northern and southern giant petrels tracked during the incubation and brood-guard periods in November 2022 to early March 2023 at Bird Island (South Georgia). The lines represent the predicted responses for each sex and the shading represents the 95% confidence interval. The top and bottom panes show the predicted flapping rates relative to wind speed with swell held at the median value, and the predicted flapping rates relative to swell height with wind speed held at the median value, respectively.

male giant petrels if they followed the tracks of females, or if they followed the tracks of males ($p < 0.001$, Dunn-Šidák correction; Figure S5). Table S3 gives a full summary of the comparisons made in predicted flapping rates between sexes.

3.6 | Suitable habitat for soaring

Maps of potential habitat for soaring giant petrels derived from our models suggest that optimal habitat extends further north for female northern than female southern giant petrels, and is more extensive for female than male southern giant petrels (Figure 6). Areas of potential habitat suitable for soaring 50% of the time were considerably larger for female than male southern giant petrels, and highest for female northern giant petrels (Table 2).

4 | DISCUSSION

Most studies of dynamic soaring behaviour and its relationship to wind have been in albatrosses rather than in petrels. Previous observational studies of giant petrels highlighted the importance of dynamic soaring behaviour (Obst & Nagy, 1992; Pennycuick, 1982), but until our study there were no detailed analyses of their flight or energy expenditure in relation to wind or waves. Using high-resolution accelerometry and GPS data, our study is the first to quantify the importance of both wind and waves in determining flight energetics for giant petrels. We show that wind and waves may be used additively to reduce flapping rates, and that the interaction between these variables and morphology may explain the marked sexual segregation in habitat use in the two species.

We found that both male and female northern and southern giant petrels reduced flapping rates with increasing wind speed, reducing energy expenditure while dynamic soaring. Our results also suggest that waves affect flight energetics; flapping rates declined with increasing swell height, indicating that giant petrels can use wave slope soaring to reduce the energetic cost of travel. Models that incorporated both wind speed and swell height best explained flapping rates, with the lowest flapping rates recorded when both wind speed and swell were high; indeed, higher wind and waves together reduced flapping by 76% to 91%, reflecting marked energy savings. The upper end of this range is comparable to the reduction in energy expenditure through wind and waves of 89–93% in albatrosses (Maywar et al., 2025), which are considered to be soaring specialists (Pennycuick, 1982; Richardson, 2011).

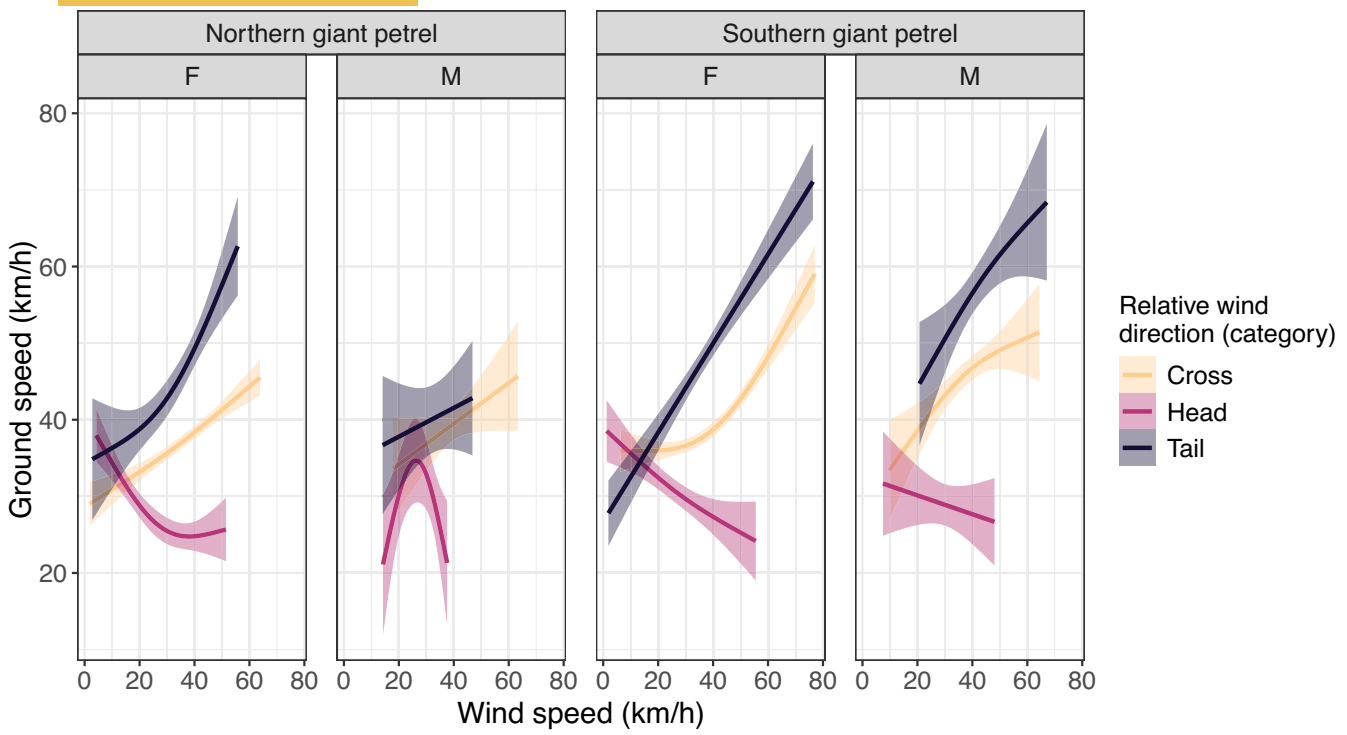

FIGURE 5 Plots showing average ground speed relative to wind speed and categorical wind direction in giant petrels tracked during incubation and brood-guard in November 2022 to early March 2023 at Bird Island (South Georgia). The lines represent the average ground speed in different categories of relative wind direction (headwind, crosswind and tailwind), and the shading represents the 95% confidence interval.

Our results demonstrate that morphology modulates the relationship between wind, waves and flight efficiency. Though male and female giant petrels have similar aspect ratios, male giant petrels at Bird Island are 41–43% heavier during the brood-guard period, and have a 15–16% higher wing loading than females. These differences in morphology have important implications for the energetic cost of travel. Birds with higher wing loadings attain higher ground speeds while gliding (Dehnhard et al., 2021; Wakefield et al., 2009), and this was apparent when comparing average ground speeds between species and sexes in our study (Table 1). However, flight theory suggests that a higher wing loading also limits the range of airspeeds that allow dynamic soaring, because higher airspeeds are needed to generate lift and for birds to stay aloft when gliding (Pennycuick, 2008). Of the various metrics of aerodynamic performance, stalling speed has the greatest impact on soaring ability because birds cannot achieve gliding flight below the stalling speed unless flying at a very steep angle of descent (Pennycuick, 2008). As a result, birds with high wing loadings, and therefore high stalling speeds, cannot maximize energy capture while dynamic soaring (i.e. cannot use low travel speeds, which minimize the vertical component of the dynamic soaring arc) to the same extent as birds with lower wing loadings but otherwise similar wing morphology (i.e. aspect ratio). We calculated that stalling speeds were only ~7% higher in male than female giant petrels, but this may translate to a considerable disadvantage in terms of flight energetic efficiency. This is supported by our observational data which suggest—given their higher flapping rates—that male giant petrels were less efficient at dynamic soaring than females (Table 1). Indeed, females had lower flapping rates throughout the range of observed wind speeds and swell heights (Figure 2). Further, when we predicted how frequently males would have to flap if they were to follow the same foraging routes as females (i.e. experience the same wind and wave conditions), and vice versa (females following the tracks of males), we found that males would incur a considerably higher energetic cost (more flaps) (Table S3). Indeed, across all our analyses, differences in flight energetics were greater between sexes than between species.

The differences in morphology and influence on flight energetics appear to play a role in explaining the striking sexual segregation in habitat use in giant petrels for most of the breeding season; male giant petrels feed to a much greater extent on carrion and other prey on land, whereas females feed much further out at sea (González-Solís et al., 2000a, 2000b; Granroth-Wilding & Phillips, 2019; Hunter, 1983; Phillips et al., 2011; Reisinger et al., 2020; Thiers et al., 2014). Male giant petrels also feed further offshore in the non-breeding season and are generally more flexible in their foraging strategies (González-Solís et al., 2000b; González-Solís et al., 2008; Granroth-Wilding & Phillips, 2019). Other ecological factors, such as the seasonal decline in carrion availability that follows the end of the pupping period of Antarctic fur seals (*Arctocephalus gazella*; Hunter, 1983; Phillips et al., 2011), contribute to temporal variation in sexual segregation during breeding, but here we focus on the mechanistic links between the environment (i.e. wind and waves) and energetics.

TABLE 2 Metrics describing the spatial extent of suitable habitat for soaring in giant petrels.

Sex and species	Total area (km^2) of suitable soaring habitat (over 0.5 threshold)	Proportion of available habitat in study area (over 0.5 threshold)
Female northern giant petrel	13,414,221	0.47
Female southern giant petrel	9,328,511	0.34
Male southern giant petrel	3,939,821	0.14

Note: Includes the total area (km^2) and the proportion of habitat within the study region (defined as the minimum and maximum latitude and longitude travelled by all birds in the study, respectively) suitable for soaring during at least 50% of hours during the middle month of incubation (November, 2022 for northern giant petrels, and December, 2022 for southern giant petrels).

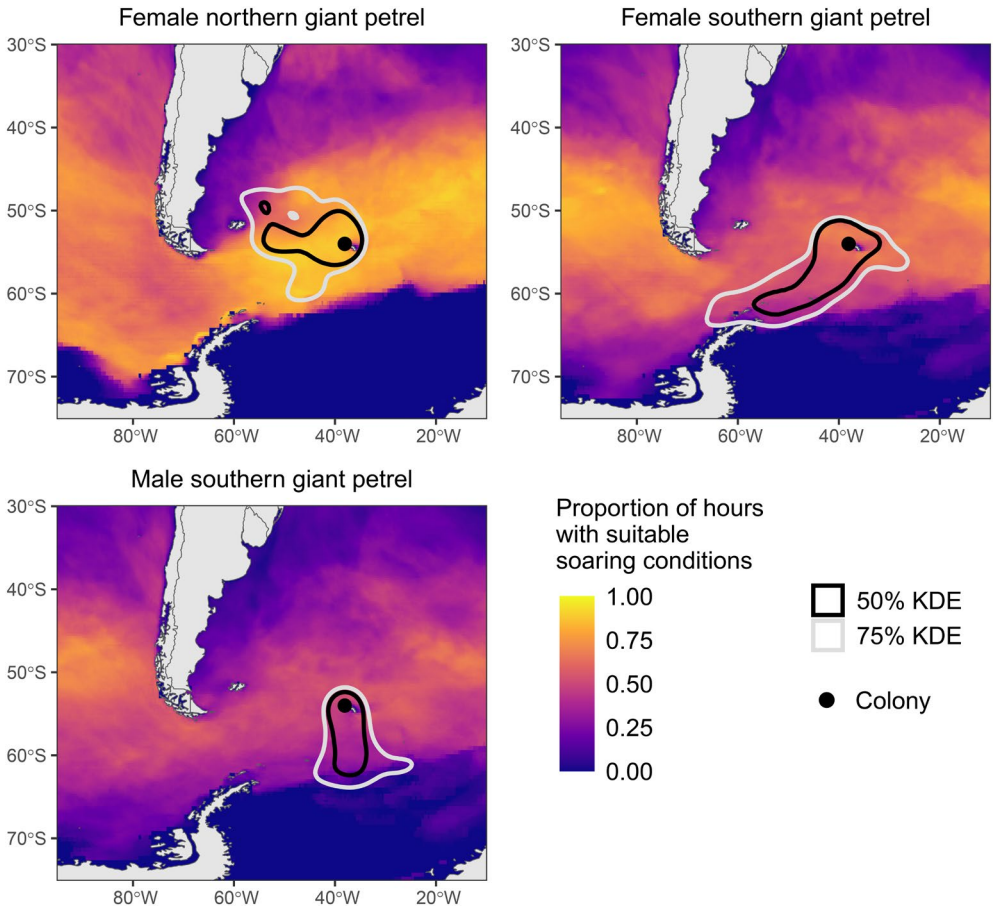

FIGURE 6 Maps showing the proportion of hours with suitable soaring conditions based on wind speed and swell height during the middle month of incubation of northern (November, 2022) and southern giant petrels (December, 2022) tracked at Bird Island (South Georgia).

Several explanations have been proposed for the marked sexual segregation in giant petrels, including reduced intraspecific competition, given the much larger body size of males and dominance at carcasses (González-Solís, 2004; González-Solís et al., 2000a; Granroth-Wilding & Phillips, 2019; Hunter, 1983; Reisinger et al., 2020; Thiers et al., 2014). It has also been suggested that their larger size leads to a higher energetic cost for males during offshore foraging trips (González-Solís et al., 2000b). Our maps of suitable habitat for soaring, as well as the comparisons of wind and waves experienced by each sex, suggest that the ability to fly efficiently may constrain the distribution of male giant petrels more than females. Female giant petrels used regions with low wind speeds (< 20 km/h) more frequently than males, and the size of the predicted areas that were suitable for soaring for 50% of the time based on wind and swell were much larger (by 2.4 times in southern giant petrels; Table 2). Based on our models, males require higher wind speeds than females for gliding flight, and hence may avoid travelling offshore if environmental conditions are not conducive to soaring flight.

Our findings suggest that giant petrels maximize time in cross- and tailwinds due to benefits in terms of both energy expenditure and travel speed. Previous studies suggested that birds are more likely

to utilize dynamic soaring in crosswinds and tailwinds (De Pascalis et al., 2020; Gibb et al., 2017), because flying is more costly in headwinds (Richardson et al., 2018; Weimerskirch et al., 2000), and because the effects of wind speed on ground speed are dependent on wind direction (Harris et al., 2025; Spear & Ainley, 1997b). We demonstrate that, in addition to increasing ground speed, use of cross- and tailwinds reduces energy expenditure in giant petrels. Thus, giant petrels likely avoid travelling in headwinds due to both the increased energetic cost of travel and the decreased ground speed.

Advancements in biologging technology and the availability of global environmental data in recent decades have greatly improved our understanding of how wind influences seabird energetics and movement, even if many questions remain (Thorne et al., 2023). Our study demonstrates the advantages of combining accelerometry and GPS data with metrics of aerodynamic efficiency to quantify the energetic responses of seabirds to environmental variability. We highlight how morphology, wind and waves combine to influence energetics of flight in giant petrels and suggest how these factors could constrain their at-sea distribution and partly explain sexual segregation during the breeding season. The Southern Ocean westerly winds are projected to shift poleward (Goyal et al., 2021; Toggweiler, 2009), which will influence wind regimes, including the regions where wind speeds are high within foraging distances of giant petrels and other seabirds breeding on subantarctic islands and in Antarctica. There is ample evidence that changing wind conditions affect breeding success and population dynamics of seabirds in general (Thorne et al., 2023). Understanding the interplay of these factors is important for predicting changes in habitat use and energetics of giant petrels and other seabirds under future climate change, which can ultimately guide management decisions to improve their conservation.

AUTHOR CONTRIBUTIONS

Madeline Hallet, Richard Phillips and Lesley Thorne conceived the ideas and designed methodology; Richard Phillips oversaw data collection efforts; Madeline Hallet, Lesley Thorne, and Richard Phillips curated the data; Madeline Hallet processed and analysed the data; Lesley Thorne oversaw progress and analyses; Ian Maywar contributed to processing and analysis code; Madeline Hallet and Lesley Thorne led the writing of the manuscript. All authors contributed critically to the drafts and gave final approval for publication.

ACKNOWLEDGEMENTS

We are very grateful to Imogen Lloyd and Mark Whiffin for carrying out the fieldwork at Bird Island. We thank Chelsi Napoli and Nathan Hirtle for their help with model design and feedback on statistical analyses.

FUNDING INFORMATION

Funding for fieldwork was provided by a National Science Foundation (NSF) CAREER award to Lesley Thorne (award no. 79804), and Natural Environment Research Council core funding to the Ecosystems CONSEC programme at British Antarctic Survey as part of the Polar Science for a Sustainable Planet science strategy. Funding for analyses was provided by a NSF award to Lesley Thorne and Richard Phillips (award no. 2444342).

CONFLICT OF INTEREST STATEMENT

The authors declare that they have no conflicts of interest.

DATA AVAILABILITY STATEMENT

All data used to produce models are available from the Dryad Digital Repository: https://doi.org/10.5061/dryad.pk0p2nh48 (Hallet et al., 2026).

ORCID

Madeline E. Hallet https://orcid.org/0009-0008-4919-7904
Ian J. Maywar https://orcid.org/0000-0003-4331-3018
Lesley H. Thorne https://orcid.org/0000-0002-6297-0091

REFERENCES

Baines, A. (1889). The sailing flight of the albatross. *Nature*, *40*, 9–10. https://doi.org/10.1038/040009b0

Bousquet, G. D., Triantafyllou, M. S., & Slotine, J.-J. E. (2017). Optimal dynamic soaring consists of successive shallow arcs. *Journal of the Royal Society Interface*, *14*(135), 20170496. https://doi.org/10.1098/rsif.2017.0496

Butler, P. J. (1991). Exercise in birds. *The Journal of Experimental Biology*, *160*, 233–262. https://doi.org/10.1242/jeb.160.1.233

Collins, P. M., Green, J. A., Elliott, K. H., Shaw, P. J. A., Chivers, L., Hatch, S. A., & Halsey, L. G. (2020). Coping with the commute: Behavioural responses to wind conditions in a foraging seabird. *Journal of Avian Biology*, *51*(4). https://doi.org/10.1111/jav.02057

Cone, C. D. (1964). A mathematical analysis of the dynamic soaring flight of the albatross with ecological interpretations. Virginia Institute of Marine Science Special Scientific Report no. 50. https://doi.org/10.21220/V5P88C

Conners, M., Michelot, T., Heywood, E. I., Orben, R. A., Phillips, R. A., Vyssotski, A., Shaffer, S. A., & Thorne, L. H. (2021). Hidden Markov models identify major movement modes in accelerometer and magnetometer data from four albatross species. *Movement Ecology*, *9*(7), 7. https://doi.org/10.1186/s40462-021-00243-z

Conners, M. G., Green, J. A., Phillips, R. A., Orben, R. A., Cui, C., Djurić, P. M., Heywood, E., Vyssotski, A. L., & Thorne, L. H. (2024). Dynamic soaring decouples dynamic body acceleration and energetics in albatrosses. *Journal of Experimental Biology*, *227*(18). https://doi.org/10.1242/jeb.247431

Copernicus Climate Change Service. (2023). ERA5 hourly data on single levels from 1940 to present. *Copernicus climate change service (C3S) climate data store (CDS)*. https://doi.org/10.24381/cds.adbb2d47

da Vinci, L. (1505). Codex on the flight of birds. Biblioteca Reale, Turin, Italy. Retrieved from the Library of Congress, https://www.loc.gov/item/2021668201/

De Pascalis, F., Imperio, S., Benvenuti, A., Catoni, C., Rubolini, D., & Cecere, J. G. (2020). Sex-specific foraging behaviour is affected by wind conditions in a sexually size dimorphic seabird. *Animal Behaviour*, *166*, 207–218. https://doi.org/10.1016/j.anbehav.2020.05.014

Dehnhard, N., Klekociuk, A. R., & Emmerson, L. (2021). Interactive effects of body mass changes and species-specific morphology on flight behavior of chick-rearing Antarctic fulmarine petrels under diurnal wind patterns. *Ecology and Evolution*, *11*(9), 4972–4991. https://doi.org/10.1002/ece3.7501

Gibb, R., Shoji, A., Fayet, A. L., Perrins, C. M., Guilford, T., & Freeman, R. (2017). Remotely sensed wind speed predicts soaring behaviour in a wide-ranging pelagic seabird. *Journal of the Royal Society Interface*, *14*(132), 20170262. https://doi.org/10.1098/rsif.2017.0262

González-Solís, J. (2004). Sexual size dimorphism in northern giant petrels: Ecological correlates and scaling. *Oikos*, *105*(2), 247–254. https://doi.org/10.1111/j.0030-1299.2004.12997.x

González-Solís, J., Croxall, J. P., & Afanasyev, V. (2008). Offshore spatial segregation in giant petrels *Macronectes spp.*: Differences between species, sexes and seasons. *Aquatic Conservation*, *17*(S1), S22–S36. https://doi.org/10.1002/aqc.911

González-Solís, J., Croxall, J. P., & Wood, A. G. (2000a). Foraging partitioning between giant petrels *Macronectes* spp. and its relationship with breeding population changes at Bird Island, South Georgia. *Marine Ecology Progress Series*, *204*, 279–288. https://doi.org/10.3354/meps204279

González-Solís, J., Croxall, J. P., & Wood, A. G. (2000b). Sexual dimorphism and sexual segregation in foraging strategies of northern giant petrels, Macronectes halli, during incubation. *Oikos*, *90*(2), 390–398. https://doi.org/10.1034/j.1600-0706.2000.900220.x

Goyal, R., Gupta, A. S., Jucker, M., & England, M. H. (2021). Historical and projected changes in the southern hemisphere surface westerlies. *Geophysical Research Letters*, *48*, e2020GL090849. https://doi.org/10.1029/2020GL090849

Granroth-Wilding, H. M. V., & Phillips, R. A. (2019). Segregation in space and time explains the coexistence of two sympatric sub-Antarctic petrels. *Ibis (London, England)*, *161*(1), 101–116. https://doi.org/10.1111/ibi.12584

Hallet, M., Thorne, L., & Phillips, R. (2026). Data from: Wind, waves, wing loading and the flight energetics of giant petrels [Dataset]. Dryad. https://doi.org/10.5061/dryad.pk0p2nh48

Harris, S. M., Bishop, C. M., Bond, S., Fernandes, P. G., Guilford, T., Lewin, P. J., Padget, O., Robins, P., Schneider, W. T., Waggitt, J. J., Wilmes, S. B., & Cordes, L. S. (2025). Adjustable wind selectivity in shearwaters implies knowledge of the foraging landscape. *Current Biology*, *35*(4), 889–897.e3. https://doi.org/10.1016/j.cub.2024.12.017

Hedenström, A. (2003). Twenty-three testable predictions about bird flight. In P. Berthold, E. Gwinner, & E. Sonnenschein (Eds.), *Avian migration* (pp. 563–582). Springer. https://doi.org/10.1007/978-3-662-05957-9_38

Hernangómez, D. (2023). Using the tidyverse with terra objects: The tidyterra package. *The Journal of Open Source Software*, *8*(91), 5751. https://doi.org/10.21105/joss.05751

Hersbach, H., Bell, B., Berrisford, P., Biavati, G., Horányi, A., Muñoz Sabater, J., Nicolas, J., Peubey, C., Radu, R., Rozum, I., Schepers, D., Simmons, A., Soci, C., Dee, D., & Thépaut, J.-N. (2023). ERA5 hourly data on single levels from 1940 to present. *Copernicus Climate Change Service (C3S) Climate Data Store (CDS)*. https://doi.org/10.24381/cds.adbb2d47

Hunter, S. (1983). The food and feeding ecology of the giant petrels *Macronectes halli* and *M. giganteus* at South Georgia. *Journal of Zoology (1987)*, *200*(4), 521–538. https://doi.org/10.1111/j.1469-7998.1983.tb02813.x

Hunter, S. (1984). Breeding biology and population dynamics of giant petrels *Macronectes* at South Georgia (Aves: Procellariiformes). *Journal of Zoology*, *203*, 441–460. https://doi.org/10.1111/j.1469-7998.1984.tb02343.x

Kemp, M. U., Shamoun-Baranes, J., Van Gasteren, H., Bouten, W., & Van Loon, E. E. (2010). Can wind help explain seasonal differences in avian migration speed. *Journal of Avian Biology*, *41*(6), 672–677. https://doi.org/10.1111/j.1600-048X.2010.05053.x

Kempton, J. A., Wynn, J., Bond, S., Evry, J., Fayet, A. L., Gillies, N., Guilford, T., Kavelaars, M., Juarez-Martinez, I., Padget, O., Rutz, C., Shoji, A., Syposz, M., & Taylor, G. K. (2022). Optimization of dynamic soaring in a flap-gliding seabird affects its large-scale distribution at sea. *Science Advances*, *8*(22), eabo0200. https://doi.org/10.1126/sciadv.abo0200

Kogure, Y., Sato, K., Watanuki, Y., Wanless, S., & Daunt, F. (2016). European shags optimize their flight behavior according to wind conditions. *Journal of Experimental Biology*, *219*(3), 311–318. https://doi.org/10.1242/jeb.131441

Lotz, S. I., & Clilverd, M. (2019). Demonstrating the use of a class of min-max smoothers for D region event detection in narrow band VLF phase. *Radio Science*, *54*, 233–244. https://doi.org/10.1029/2018RS006701

Maywar, I. J., Phillips, R. A., Orben, R. A., Conners, M. G., Shaffer, S. A., & Thorne, L. H. (2025). Differential impacts of wind and waves on albatross flight performance in two ocean basins. *Movement Ecology*, *14*(1), 1. https://doi.org/10.1186/s40462-025-00614-w

Michelot, T., Langrock, R., & Patterson, T. A. (2016). moveHMM: An R package for the statistical modelling of animal movement data using hidden Markov models. *Methods in Ecology and Evolution*, *7*(11), 1308–1315. Portico. https://doi.org/10.1111/2041-210x.12578

Obst, B. S., & Nagy, K. A. (1992). Field energy expenditures of the southern giant-petrel. *The Condor*, *94*(4), 801–810. https://doi.org/10.2307/1369278

Parrott, G. C. (1970). Aerodynamics of gliding flight of a black vulture *Coragyps atratus*. *Journal of Experimental Biology*, *53*(2), 363–374. https://doi.org/10.1242/jeb.53.2.363

Pennycuick, C. J. (1978). Fifteen testable predictions about bird flight. *Oikos*, *30*(2), 165–176. https://doi.org/10.2307/3543476

Pennycuick, C. J. (1982). The flight of petrels and albatrosses (Procellariiformes), observed in South Georgia and its vicinity. *Philosophical Transactions of the Royal Society of London. B, Biological Sciences*, *300*(1098), 75–106. https://doi.org/10.1098/rstb.1982.0158

Pennycuick, C. J. (2008). *Modelling the flying bird*, *theoretical ecology series*. Academic Press.

Phillips, R. A., McGill, R. A. R., Dawson, D. A., & Bearhop, S. (2011). Sexual segregation in distribution, diet and trophic level of seabirds: Insights from stable isotope analysis. *Marine Biology*, *158*, 2199–2208. https://doi.org/10.1007/s00227-011-1725-4

Phillips, R. A., Xavier, J. C., & Croxall, J. P. (2003). Effects of satellite transmitters on albatrosses and petrels. *Auk*, *120*(4), 1082–1090. https://doi.org/10.1093/auk/120.4.1082

Rayleigh, J. W. S. (1883). The soaring of birds. *Nature*, *27*, 534–535. https://doi.org/10.1038/027534a0

Reisinger, R. R., Carpenter-Kling, T., Connan, M., Cherel, Y., & Pistorius, P. A. (2020). Foraging behaviour and habitat-use drives niche segregation in sibling seabird species. *Royal Society Open Science*, *7*(9), 200649. https://doi.org/10.1098/rsos.200649

Richardson, P. L. (2011). How do albatrosses fly around the world without flapping their wings? *Progress in Oceanography*, *88*(1–4), 46–58. https://doi.org/10.1016/j.pocean.2010.08.001

Richardson, P. L. (2018). Leonardo da Vinci's discovery of the dynamic soaring by birds in wind shear. *Notes and Records of the Royal Society of London*, *73*(3), 285–301. https://doi.org/10.1098/rsnr.2018.0024

Richardson, P. L., Wakefield, E. D., & Phillips, R. A. (2018). Flight speed and performance of the wandering albatross with respect to wind. *Movement Ecology*, *6*, 3. https://doi.org/10.1186/s40462-018-0121-9

Sachs, G. (2005). Minimum shear wind strength required for dynamic soaring of albatrosses. *Ibis*, *147*(1), 1–10. https://doi.org/10.1111/j.1474-919x.2004.00295.x

Safi, K., Kranstauber, B., Weinzierl, R., Griffin, L., Rees, E. C., Cabot, D., Cruz, S., Proaño, C., Takekawa, J. Y., Newman, S. H., Waldenström, J., Bengtsson, D., Kays, R., Wikelski, M., & Bohrer, G. (2013). Flying with the wind: Scale dependency of speed and direction measurements in modelling wind support in avian flight. *Movement Ecology*, *1*(1), 4. https://doi.org/10.1186/2051-3933-1-4

Sato, K., Sakamoto, K. Q., Watanuki, Y., Takahashi, A., Katsumata, N., Bost, C.-A., & Weimerskirch, H. (2009). Scaling of soaring seabirds

and implications for flight abilities of Giant pterosaurs. *PLoS One*, *4*, e5400. https://doi.org/10.1371/journal.pone.0005400

Schoombie, S., Wilson, R., & Ryan, P. (2023). Wind driven effects on the fine-scale flight behaviour of dynamic soaring wandering albatrosses. *Marine Ecology. Progress Series (Halstenbek)*, *723*, 119–134. https://doi.org/10.3354/meps14265

Spear, L. B., & Ainley, D. G. (1997a). Flight behaviour of seabirds in relation to wind direction and wing morphology. *Ibis*, *139*, 221–233. https://doi.org/10.1111/j.1474-919X.1997.tb04620.x

Spear, L. B., & Ainley, D. G. (1997b). Flight speed of seabirds in relation to wind speed and direction. *Ibis*, *139*, 234–251. https://doi.org/10.1111/j.1474-919X.1997.tb04621.x

Spivey, R. J., Stansfield, S., & Bishop, C. M. (2014). Analysing the intermittent flapping flight of a Manx shearwater, *Puffinus puffinus*, and its sporadic use of a wave-meandering wing-sailing flight strategy. *Progress in Oceanography*, *125*, 62–73. https://doi.org/10.1016/j.pocean.2014.04.005

Stokes, I. A., & Lucas, A. J. (2021). Wave-slope soaring of the brown pelican. *Movement Ecology*, *9*, 13. https://doi.org/10.1186/s40462-021-00247-9

Suryan, R. M., Anderson, D. J., Shaffer, S. A., Roby, D. D., Tremblay, Y., Costa, D. A., Sievert, P. R., Sato, F., Ozaki, K., Balogh, G. R., & Nakamura, N. (2008). Wind, waves, and wing loading: Morphological specialization may limit range expansion of endangered albatrosses. *PLoS One*, *3*(12), e4016. https://doi.org/10.1371/journal.pone.0004016

Thiers, L., Delord, K., Barbraud, C., Phillips, R. A., Pinaud, D., & Weimerskirch, H. (2014). Foraging zones of the two sibling species of giant petrels in the Indian Ocean throughout the annual cycle: Implication for their conservation. *Marine Ecology. Progress Series (Halstenbek)*, *499*, 233–248. https://doi.org/10.3354/meps10620

Thorne, L., Clay, T., Phillips, R., Silvers, L., & Wakefield, E. (2023). Effects of wind on the movement, behavior, energetics, and life history of seabirds. *Marine Ecology. Progress Series (Halstenbek)*, *723*, 73–117. https://doi.org/10.3354/meps14417

Toggweiler, J. R. (2009). Shifting westerlies. *Science*, *323*(5920), 1434–1435. https://doi.org/10.1126/science.1169823

Tucker, V. A., & Parrott, G. C. (1970). Aerodynamics of gliding flight in a falcon and other birds. *Journal of Experimental Biology*, *52*(2), 345–367. https://doi.org/10.1242/jeb.52.2.345

Wakefield, E. D., Phillips, R. A., Matthiopoulos, J., Fukuda, A., Higuchi, H., Marshall, G. J., & Trathan, P. N. (2009). Wind field and sex constrain the flight speeds of central-place foraging albatrosses. *Ecological Monographs*, *79*, 663–679. https://doi.org/10.1890/07-2111.1

Warham, J. (1977). Wing loadings, wing shapes, and flight capabilities of Procellariiformes. *New Zealand Journal of Zoology*, *4*(1), 73–83. https://doi.org/10.1080/03014223.1977.9517938

Weimerskirch, H., Guionnet, T., Martin, J., Shaffer, S. A., & Costa, D. P. (2000). Fast and fuel efficient? Optimal use of wind by flying albatrosses. *Proceedings of the Royal Society B: Biological Sciences*, *267*(1455), 1869–1874. https://doi.org/10.1098/rspb.2000.1223

Weimerskirch, H., Louzao, M., de Grissac, S., & Delord, K. (2012). Changes in wind pattern alter albatross distribution and life-history traits. *Science*, *335*(6065), 211–214. https://doi.org/10.1126/science.1210270

Wilson, J. (1975). Sweeping flight and soaring by albatrosses. *Nature*, *257*, 307–308. https://doi.org/10.1038/257307a0

Wood, S. N. (2017). *Generalized additive models: An introduction with R* (2nd ed.). CRC Press, Taylor & Francis Group. https://doi.org/10.1201/9781315370279

SUPPORTING INFORMATION

Additional supporting information can be found online in the Supporting Information section at the end of this article.

Figure S1. Boxplots of the proportion of time giant petrels spent in relative wind and wave angles. Bird-wind angles are categorized as tailwinds (<60°), crosswinds (≥60° & <120°) and headwinds (≥120°), while bird-swell angles are categorized as with (<60°), across (≥60° & <120°) and against (≥120°) the swell.

Figure S2. Boxplots of the proportion of time female giant petrels spent in different relative wind angles and wind intensities. Wind intensities are categorized as being low, medium or high, and relative wind angles are categorized as head-, cross- or tailwinds. Wind speeds were categorized such that the distribution of wind speeds experienced by all species and sexes were divided into 1/3 quantiles. Proportions are calculated within each relative wind direction category (e.g. the proportion of time in low headwinds is calculated as the time spent in low headwinds divided by total time spent in headwinds).

Figure S3. Boxplots of the proportion of time male giant petrels spent in different relative wind angles and wind intensities. Wind intensities are categorized as being low, medium or high, and relative wind angles are categorized as head-, cross- or tailwinds. Wind speeds were categorized such that the distribution of wind speeds experienced by all species and sexes were divided into 1/3 quantiles. Proportions are calculated within each relative wind direction category (e.g. the proportion of time in low headwinds is calculated as the time spent in low headwinds divided by total time spent in headwinds).

Figure S4. Flapping rates predicted from wind speed and relative wind direction of tracked female giant petrels. Models were constructed using data from northern and southern giant petrels tracked during the incubation and brood-guard periods in November 2022 to early March 2023 at Bird Island (South Georgia). The lines represent the predicted flapping responses for different relative wind directions (derived bird-wind-angle) and the shading represents the 95% confidence interval. Bird-wind angles are calculated on a 0–180° scale, such that bird-wind angles <60° represent tailwinds, bird-wind-angles ≥60° and <120° are crosswinds, and bird-wind-angles ≥120° are headwinds.

Figure S5. Boxplots of predicted flapping rates along giant petrel tracks. Flapping rates were predicted for female giant petrels and male giant petrels based on wind and wave conditions along tracks of female giant petrels, and based on wind and wave conditions along tracks of male giant petrels.

Table S1. Table summarizing the number of deployments and available data used in models. Models were constructed to predict flapping rates relative to windspeed and swell height for male and female northern and southern giant petrels tracked during the incubation and brood-guard periods in November 2022 to early March 2023 from Bird Island (South Georgia). The number of successful deployments refers to the number of birds that were deployed with tags and returned with all tags present and functioning. The number of deployments included in models refers to the number of successful deployments that were actually used when constructing the models. The mean deployment duration refers to the number of days that the tags were deployed on birds

(i.e. number of days between initial tag deployment and when the tag was removed).

Table S2. Table summarizing model performance metrics. Performance metrics are given for models of flapping rate (flaps per hour) relative to wind speed and swell height for northern and southern giant petrels tracked during the incubation and brood-guard periods in November 2022 to early March 2023 at Bird Island (South Georgia). Terms that were not significant are in grey text. Abbreviations are as follows: AICc, corrected AIC; dAICc, delta AICc; df, degrees of freedom; weight, AICc weight; DE, deviance explained. The most parsimonious models (in which deltaAICc = 0) for each species/sex are in bold text.

Table S3. Table summarizing results of predicted flapping rate comparisons between sexes. Predicted flapping rates of female giant petrels and male giant petrels were based on wind and wave conditions along tracks of female giant petrels, and based on wind and wave conditions along tracks of male giant petrels, during the incubation and brood-guard periods in November 2022 to early March 2023 at Bird Island (South Georgia). Sex (predicted flaps) refers to the sex that flapping rates are being predicted for, while Sex (tracks) refers to the tracks on which flapping rates were predicted for. All comparisons were significant (Dunn-Šidák correction for multiple comparisons: $\alpha = 0.0127$).

Table S4. Table summarizing the spatial distribution of tracked birds. Includes the minimum and maximum latitude and longitude, respectively, travelled by each species of giant petrel tracked during the incubation and brood-guard periods in November 2022 to early March 2023 at Bird Island (South Georgia). All coordinates are rounded to the nearest whole degree, and coordinates in bold text were used to define the spatial bounding box in our map of suitable habitat for soaring (slightly adjusted for visualization purposes; Figure 6), which are given in the last row.

How to cite this article: Hallet, M. E., Phillips, R. A., Maywar, I. J., & Thorne, L. H. (2026). Wind, waves, wing loading and the flight energetics of giant petrels. *Functional Ecology*, *00*, 1–15. https://doi.org/10.1111/1365-2435.70352